Available online at www.sciencedirect.com
SCIENCE DIRECT®
International Journal of Heat and Mass Transfer 48 (2005) 537–544
International Journal of HEAT and MASS TRANSFER
www.elsevier.com/locate/ijhmt

Heat transfer mechanisms in thin film with laser heat source

Shuichi Torii [a,*], Wen-Jei Yang [b,1]

[a] Department of Mechanical Engineering and Materials Science, Kumamoto University, Kumamoto 860-8555, Japan
[b] Mechanical Engineering and Applied Mechanics, The University of Michigan, Ann Arbor, MI 48109, USA

Received 15 January 2004; received in revised form 10 September 2004
Available online 11 November 2004

Abstract

The present study deals with the effect of laser radiation on the propagation phenomenon of a thermal wave in a very thin film subjected to a symmetrical heating on both sides. Pulsating laser heating is modelled as an internal heat source with various time characteristics. The Cattaneo heat flux law together with the energy conservation equation is solved by a numerical technique based on explicit scheme, i.e., MacCormack's predictor–corrector scheme. Results are obtained for the time history of heat transfer behaviour before and after symmetrical collision of wave fronts from two sides of a film. The study concludes (1) if the absorption coefficient of the continuously-operated- and pulsating-laser heat source increases, temperature overshoot causes in a very thin film within a very short period of time, and (2) the overshoot and oscillation of thermal wave depend on the frequency of the heat source time characteristics. This trend becomes minor in a thick film.

Keywords: Thermal propagation; Non-Fourier heat conduction; Relaxation time; MacCormack's predictor–corrector scheme; Laser heat source

1. Introduction

When the elapsed time during a transient is extremely short, the classical Fourier heat conduction equation breaks down at low temperature near absolute zero or at moderate temperature. That is, the thermal wave travels in the medium with a finite speed of propagation [1–4]. An increasing interest has arisen recently in the use of heat sources such as lasers and microwaves, which have found numerous applications related to material processing (e.g. surface annealing, welding and drilling of metals, sintering of ceramics, scientific research and medicine). Experimental and theoretical studies on these applications are reported by numerous investigators [5–7]. This is because when extremely short laser pulses or high frequencies are concerned, it may give inaccurate results. In particular as laser pulse duration approaches the microscopic relaxation times among different energy carries, the mechanism of radiation absorption becomes important [8,9]. The present study is focused on thermal propagation in a metal film subjected to a laser heat source.

In order to account for a finite propagation in the thermal field, a hyperbolic differential equation based on a relaxation model for heat conduction was introduced. Several authors have studied analytically the parabolic and hyperbolic models of heat conduction with the laser heat source and with a convective boundary

* Corresponding author. Tel./fax: +81 96 342 3756.
E-mail addresses: torii@mech.kumamoto-u.ac.jp (S. Torii), wjyang@engin.umich.edu (W.-J. Yang).
[1] Tel.: +1 734 764 9910; fax: +1 734 747 3170.

0017-9310/$ - see front matter © 2004 Elsevier Ltd. All rights reserved.
doi:10.1016/j.ijheatmasstransfer.2004.09.011

Nomenclature

c	speed of thermal wave (m/s)
c_0	reference speed of thermal wave (m/s)
c_p	specific heat at constant pressure (J/kg K)
g	strength of internal heat source (W/m^3)
g_0	reference capacity of internal heat source $\mathrm{Ir}(1-R)\mu$ (W/m^3)
$I(t)$	laser incident intensity (W/m^2)
Ir	arbitrary reference laser intensity (W/m^2)
k	thermal conductivity (W/Km)
k_0	reference thermal conductivity (W/K m)
$Q(\eta,\xi)$	dimensionless heat flux
$q(x,t)$	heat flux (W/m^2)
R	surface reflectance
$T(x,t)$	temperature (K)
T_0	reference temperature (K)
T_{w1}	wall temperature (K)
t	time (s)
x	space variable (m)
x_0	film thickness (m)

Greek symbols

α	thermal diffusivity, $k/(\rho c_p)$ (m^2/s)
α_0	reference thermal diffusivity (m^2/s)
β	dimensionless absorption coefficient, $2\tau\mu c_0$
ψ_0	constant coefficient related to the dimensionless strength of internal heat source, $\frac{k_0 g_0}{(T_{w1}-T_0)c_0^2\rho^2 c_p^2}$
η	dimensionless space variable
$\theta(\eta,\xi)$	dimensionless temperature
ξ	dimensionless time variable
$\phi(\xi)$	dimensionless rate of energy absorbed in the medium $I(2\tau\xi)/\mathrm{Ir}$
μ	absorption coefficient
ρ	density (kg/m^3)
τ	relaxation time α/c^2 (s)
Δ	dimensionless duration of the laser pulse
ω	frequency of a periodic heat source

Subscript

n	time level

Superscript

i	spatial location

condition [10–15]. Using both models, Kar et al. [16] studied heat conduction due to shortpulse heating for various boundary conditions. They reported that the predicted temperature distribution is substantially affected by the temperature dependent thermal properties. Lewandowska [17] also dealt with the parabolic and hyperbolic heat conduction in the one-dimensional, semi-infinite body with the insulated boundary and discussed different time characteristics of the heat source capacity. It is disclosed that (i) for small dimensionless Bouguer number the temperature distribution in the body results from the heat generation process, and (ii) the significant difference between the hyperbolic and parabolic solutions appears in only an edge of the body, where the hyperbolic temperature is higher than the parabolic one. Size effects on non-equilibrium laser heating of metal films were investigated by Qiu and Tien [18].

This paper deals with thermal wave behavior during transient heat conduction in a film (solid plate) subjected to a laser heat source with various time characteristics from both side surfaces. Emphasis is placed on the effect of the time characteristics of the laser heat source (constant, pulsed and periodic) on thermal wave propagation. Numerical solutions are obtained by means of a numerical technique based on MacCormack's predictor–corrector scheme to solve the non-Fourier, hyperbolic heat conduction equation [19].

2. Formation and numerical method

One-dimensional thermal propagation in a film with thickness of x_0 is analyzed, as shown in Fig. 1. At $t = 0$, the temperature field within the solid is uniform with a value T_0. For $t > 0$, the wall surfaces at $x = 0$ and x_0 are suddenly heated due to the laser heat source. Non-equilibrium convection and radiation are assumed to be negligible. Under these conditions and assumptions, the Fourier equation [12] and the energy equation with internal heat sources can be represented as

$$\tau\frac{\partial q}{\partial t} + q + k\frac{\partial T}{\partial x} = 0 \tag{1}$$

and

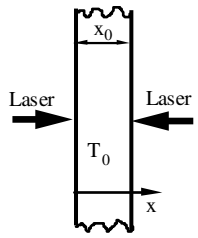

Fig. 1. Physical configuration and coordinate system.

$$\rho c_p \frac{\partial T}{\partial t} + \frac{\partial q}{\partial x} - g = 0 \tag{2}$$

respectively.

For a metal (absorption coefficient μ of the order of 10^7–$10^8\,\mathrm{m}^{-1}$) which absorbs laser energy internally, many researchers (for examples, Vick and Ozisik [10]; Ozisik and Vick [20]; Tang and Araki [21]) reported that almost all energy is absorbed within a depth of the order of 0.1 μm which can be treated as a skin effect. Thus, the model considers the laser radiation as a heat source, which is x-independent and non-zero only within a layer of the body or even as a surface heat flux. Based on this idea, the energy sources term in Eq. (2), for a material that absorbs laser energy internally, is modeled by Blackwell [11] and Zubair and Aslam [12] as

$$g(x,t) = I(t)(1-R)\mu \exp(-\mu x). \tag{3}$$

Here $I(t)$ is the laser incident intensity and R is the surface reflectance of the body. Note that this model assumes no spatial variations of $I(t)$ in the plane perpendicular to the laser beam and no heat transport in the direction perpendicular to the beam.

The following dimensionless quantities, i.e., dimensionless temperature, dimensionless heat flux, and dimensionless time and space variables are introduced as

$$\theta(\xi,\eta) = \frac{T - T_0}{T_{w1} - T_0} \tag{4a}$$

$$Q(\xi,\eta) = \frac{\alpha_0 q}{(T_{w1} - T_0)k_0 c_0}. \tag{4b}$$

$$\xi = \frac{c_0^2 t}{2\alpha_0} \tag{4c}$$

$$\eta = \frac{c_0 x}{2\alpha_0} = \frac{x}{2\tau c_0}. \tag{4d}$$

Eqs. (1) and (2) are expressed in terms of the above dimensionless variables as

$$\frac{\partial Q}{\partial \xi} + \frac{\partial \theta}{\partial \eta} + 2Q = 0 \tag{5}$$

and

$$\frac{\partial Q}{\partial \eta} + \frac{\partial \theta}{\partial \xi} - 2\psi_0 \phi(\xi)\exp(-\beta\eta) = 0. \tag{6}$$

Initial and boundary conditions are represented, as

$$\begin{aligned} &\theta = 0,\ Q = 0 \quad \text{at } \xi = 0,\ 0 < \eta < \frac{c_0 x_0}{2\alpha_0} \\ &\frac{\partial \theta}{\partial \eta} = 0,\ Q = 0 \quad \text{at } \xi > 0,\ \eta = 0 \text{ and } \frac{c_0 x_0}{2\alpha_0} \end{aligned} \tag{7}$$

Note that the boundary condition of Q at $\xi > 0$ is derived from Eqs. (5) and (6) and a minimum distance from both side walls is employed as η because of the symmetrical heating.

Glass et al. [22,23] reported that MacCormack's method [24], which is a second-order accurate explicit scheme, can handle these moving discontinuities quite well and is valid for the hyperbolic heat conduction problems. Since the hyperbolic problems considered here have step discontinuities at the thermal wave front, MacCormack's predictor–corrector scheme is used in the present study. When MacCormack's method is applied to Eqs. (5) and (6), the following finite difference formulation results:

Predictor:

$$\overline{\theta_i^{n+1}} = \theta_i^n - \frac{\Delta\xi}{\Delta\eta}(Q_{i+1}^n - Q_i^n) + \Delta\xi[-2\psi_0\phi(\Delta\xi n) \times \exp(-2\beta\Delta\eta \mathrm{i})]. \tag{8}$$

$$\overline{Q_i^{n+1}} = Q_i^n - \frac{\Delta\xi}{\Delta\eta}(\theta_{i+1}^n - \theta_i^n) - 2\Delta\xi Q_i^n \tag{9}$$

Corrector:

$$\theta_i^{n+1} = \frac{1}{2}\left\{\theta_i^n + \overline{\theta_i^{n+1}} - \frac{\Delta\xi}{\Delta\eta}\left(\overline{Q_i^{n+1}} - \overline{Q_{i-1}^{n+1}}\right) + \Delta\xi[-2\psi_0\phi((n+1)\Delta\xi)\exp(-\beta\Delta\eta i)]\right\} \tag{10}$$

$$Q_i^{n+1} = \frac{1}{2}\left[Q_i^n + \overline{Q_i^{n+1}} - \frac{\Delta\xi}{\Delta\eta}\left(\overline{\theta_i^{n+1}} - \overline{\theta_{i-1}^{n+1}}\right) - 2\Delta\xi\overline{Q_i^{n+1}}\right], \tag{11}$$

where the subscript i denotes the grid points in the space domain, superscript n denotes the time level, and $\Delta\eta$ and $\Delta\xi$ are the space and time steps, respectively. The terms with overbars, i.e., $\overline{Q_i^{n+1}}, \overline{\theta_i^{n+1}}$, etc. are a temporary predicted value at the time level $n+1$.

Throughout numerical calculations, the number of grids is properly selected between 1000 and 5000 to obtain a grid-independent solution, resulting in no appreciable difference between the numerical results with different grid spacing. The ranges of the parameters are non-dimensional plate thickness $c_0 x_0/\alpha = 1.0$ and 10.0, constant coefficient related to the dimensionless capacity of internal heat source $\psi_0 = 1$, dimensionless rate of energy absorbed in the medium, $\phi(\xi) = 1$, $\phi(\xi) = (1 + \sin(\omega\xi))/2$, and $\phi(\xi) = 100(\exp(-0.4\xi) - \exp(-0.41\xi)) - 0.3134(\xi/\Delta)^2$, and dimensionless absorption coefficients $\beta = 1$ and 10. Note that for a pulsating laser source, the same model proposed by Lewandowska [17] is employed here as follows.

$$\begin{aligned} &\phi(\xi) = 100(\exp(-0.4\xi) - \exp(-0.41\xi)) - 0.3134(\xi/\Delta)^2 \\ &\quad \text{for } \xi < \Delta \\ &\phi(\xi) = 0 \quad \text{for } \xi \geqslant \Delta \end{aligned} \tag{12}$$

In order to verify the numerical method and to determine the reliability of the computer program, numerical predictions are compared with analytical results

obtained by Lewandowska [17], who investigates the thermal waves propagating in the one-dimensional semi-infinite body with the insulated boundary. Numerical results are obtained for metals putting $\phi(\xi) = 1$ and $\psi_0 = 1$. Here, typical values of the model parameters for many metals are employed as: the thermal diffusivity α is approximately $10^{-5}\,m^2/s$ during the initial stages of laser irradiation, the relaxation time τ is the order of $10^{-11}\,s$ [25], the thermal wave speed C is the order of $10^3\,m/s$ using the correlation $\alpha = C^2\tau$, the absorption coefficient μ is typically the order of 10^7–$10^8\,m^{-1}$ and the surface reflectance of the typical metal R is about 0.9 [26].

Fig. 2, for $\beta = 1$, depicts the time history of the dimensionless temperature distribution at different locations of the body. The effect of absorption coefficient of material, β, on the temperature distribution in a plate is illustrated in Fig. 3 for $\xi = 1$. For comparison, analytical result of Lewandowska [17] is superimposed in the figure with solid lines. It is observed in Figs. 2 and 3 that the heat production is concentrated at the edge of the body, as mentioned previously. Both figures show an excellent agreement between both the present and existing solutions. The validity of the computer program and the verification of the numerical method are born out through the above comparisons.

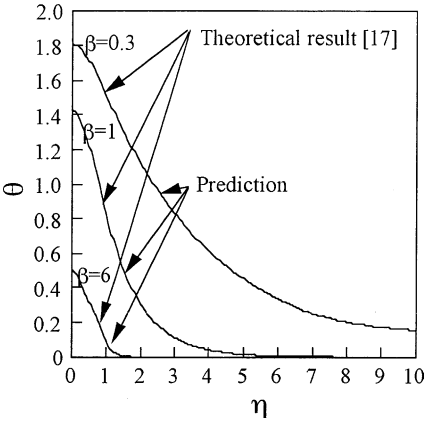

Fig. 2. A comparison of analytical results and theoretical data [17] for temperature distributions in a film for $\phi(\tau) = 1$, $\psi_0 = 1$ and $\beta = 1$.

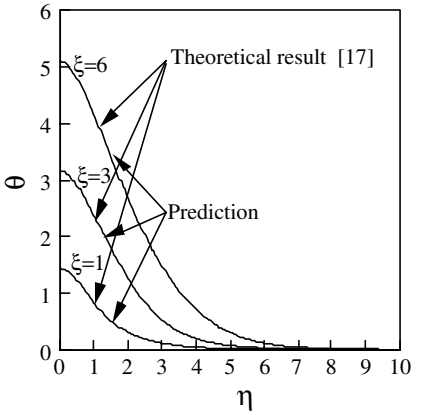

Fig. 3. A comparison of analytical results and theoretical data [17] for temperature distributions in a film for $\phi(\tau) = 1$, $\psi_0 = 1$ and $\tau = 1$.

3. Numerical results and discussion

3.1. Continuous operated laser source

Fig. 4(a) and (b), for $\phi(\xi) = 1$, $\psi_0 = 1$, and $c_0x_0/\alpha = 1.0$, depicts the time-histories of the temperature distribution, θ, in a film for $\beta = 1$ and 10, respectively. Since the space region of the heat source capacity increases for larger β, an increase in the film temperature yields over the whole film, as seen in Fig. 4(a). Note that at ξ fixed, the film temperature for $\beta = 1$ is higher than that for $\beta = 10$. It is observed in Fig. 4(b) that as time progresses,

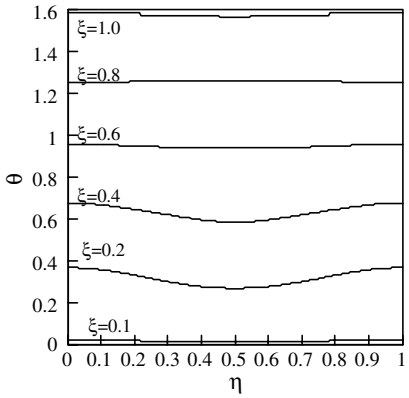

(a) β=1

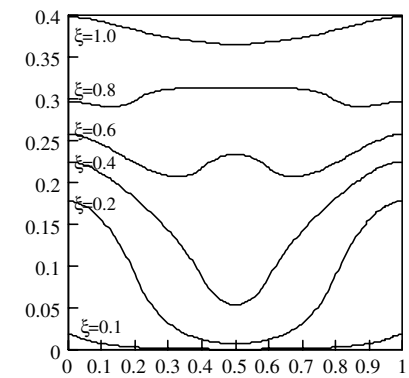

(b) β=10

Fig. 4. Instantaneous dimensionless temperature distributions in the film for $\phi(\xi) = 1$, $\psi_0 = 1$ and $c_0x_0/\alpha = 1.0$.

the film temperature for $\beta = 10$ gradually increases because almost all energy is absorbed in the vicinity of both side walls and after $\xi = 0.6$, the film temperature substantially induces in the centre region of the film, that is the temperature overshoot occurs. This trend becomes minor in a thick film, as seen in Fig. 5. Fig. 5 illustrates the time-histories of the temperature distribution, θ, in a film for $c_0x_0/\alpha = 10.0$. Notice that $\phi(\xi)$ and ψ_0 are the same as the corresponding values in Fig. 4. The film temperature gradually increases in the absence of temperature overshoot even for different β. The temperature profiles behave like diffusion domination and are in accordance with theoretical results predicted by the classical heat-conduction theory.

Next is to investigate the effect of time-dependence of laser heat source on the time history of the film temperature, for $\psi_0 = 1$ and $\beta = 10.0$. Fig. 6 illustrates the time-history of the temperature distribution in the film with $c_0x_0/\alpha = 1$, in which the periodic laser source is modeled

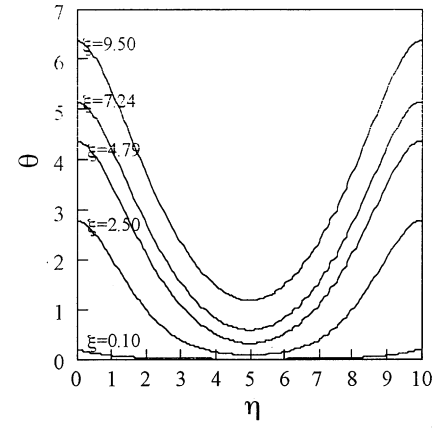

(a) β=1

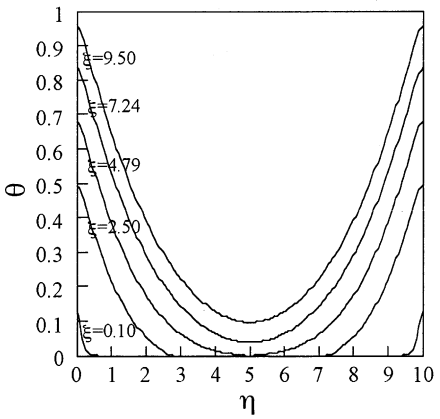

(b) β=10

Fig. 5. Instantaneous dimensionless temperature distributions in the film for $\phi(\xi) = 1$, $\psi_0 = 1$ and $c_0x_0/\alpha = 10.0$.

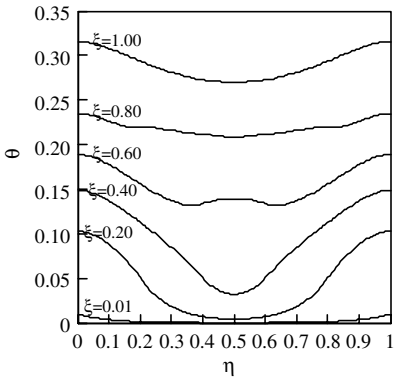

(a) ω=1

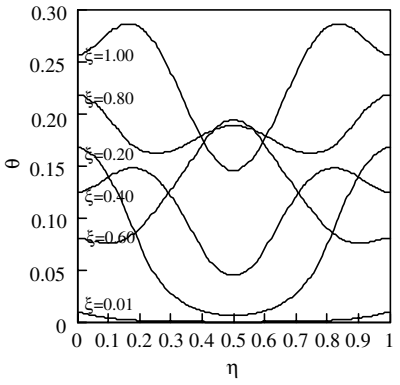

(b) ω=10

Fig. 6. Instantaneous dimensionless temperature distributions in the film for $\phi(\xi) = 1$, $\psi_0 = (1 + \sin(\omega\xi))/2$ and $c_0x_0/\alpha = 1.0$.

as $\phi\ (\xi) = (1 + \sin\omega\xi)/2$. This phenomenon implies that the heat source is periodically oscillated in the vicinity of both side-walls of the film. (a) and (b) of the figure depict numerical results for $\omega = 1$ and 10, respectively. It is observed in Fig. 6(a) that although the propagation process of thermal waves in a film, for $\omega = 1$, is similar to the numerical result for constant laser source source, as seen in Fig. 4(b), the temperature overshoot disappears. By contrast, Fig. 6(b) shows that when the frequency of the periodic laser heat source becomes larger, a substantial change in wave propagation is caused through time. One observes that (i) when wavefronts from both sides arrive at the center of the film, the temperature is substantially increased and; (ii) the temperature overshoot takes place; and (iii) thought the film temperatures at both-side walls are changed with time, the inner film temperature is increased over the whole region of the film as time progresses. The effect of the time-dependence of laser heat source becomes minor for the thick film, as seen in Fig. 7, which illustrates the timewise variation of the film temperature profile with $c_0x_0/\alpha = 10.0$. Here the values of ψ_0, $\phi(\xi)$, β

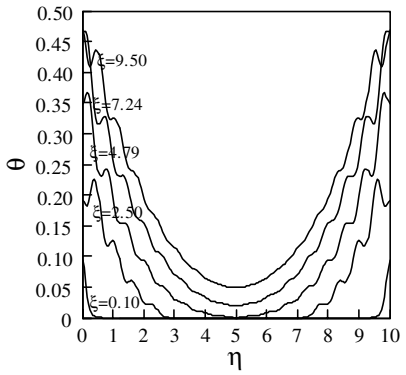

Fig. 7. Instantaneous dimensionless temperature distributions in the film for $\phi(\xi) = 1$, $\psi_0 = (1 + \sin(10\xi))/2$, $\beta = 10$ and $c_0x_0/\alpha = 10.0$.

and ω are the same as these of Fig. 6(b). One observes that as time progresses, the film temperature increases gradually, whose behavior is similar to that shown in Fig. 5(b), thought the oscillate temperature profile yields near the sidewalls because of the periodic laser heat source. Note that for the small value of β, i.e., $\beta = 1$, the calculated temperature distribution is similar to that for $\beta = 10$ (not shown), but the absolute value of the film temperature is different for $\beta = 1$ and 10. It is found that (i) the effect of the frequency of a periodic heat source ω on the temperature distribution become considerably greater in the very thin film, while its oscillation is affected only near the wall of the thick film.

3.2. Pulsed laser source

Fig. 8(a) and (b), for $c_0x_0/\alpha = 1.0$, depict the time-histories of the temperature distribution θ in a very thin film for $\Delta = 0.5$ and 5, respectively. Since the space region of the heat source capacity increases for lower β as mentioned above, an increase in the film temperature yields over the film. The film temperature, for $\Delta = 5.0$, is gradually increased over the whole cross-section of the

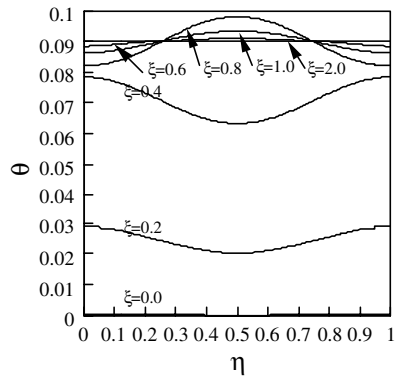

(a) Δ=0.5

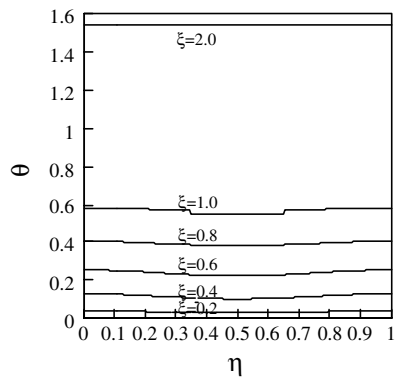

(b) Δ=5

Fig. 8. Instantaneous dimensionless temperature distributions in the film heated with a pulsating laser source for $c_0x_0/\alpha = 1.0$.

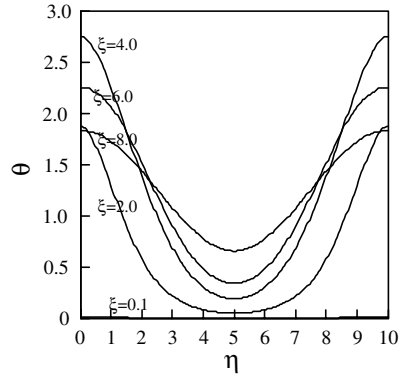

(a) Δ=5

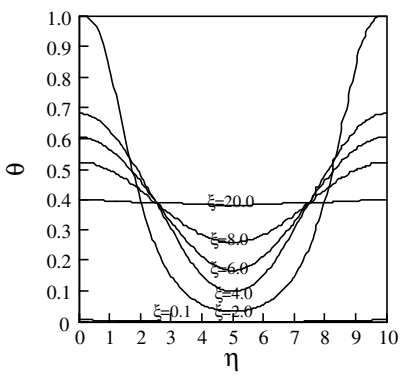

(b) Δ=2

Fig. 9. Instantaneous dimensionless temperature distributions in the film heated with a pulsating laser source for $c_0x_0/\alpha = 10.0$.

film as the time progresses (Fig. 8(b)). This is because the film is continuously heated by the laser source up to $\xi = 5.0$. In contrast, when the pulsating heat is carried out, that is when no heating is imposed in the film after $\xi = 0.5$, the substantial increase in the file temperature appears as seen in Fig. 8(a). In other words, after $\xi = 0.6$ the file temperature diminishes in the vicinity of the file surface, while the corresponding value substantially induces in the centre region of the film, that is the temperature overshoot occurs. This is because the heat propagates in the file. This trend becomes minor in a thick film, as seen in Fig. 9. Fig. 9 illustrates the time-histories of the temperature distribution, θ, in a film for $c_0 x_0/\alpha = 10.0$. (a) and (b) of Fig. 9 correspond to numerical results for $\Delta = 5$ and 2, respectively. It is observed that after the laser heating up to $\xi = 5$, the surface wall temperature diminishes, while the corresponding vale in the centre region of the film increases, as shown in Fig. 9(a). A similar thermal behavior is observed in the case of $\Delta = 2$, as seen in Fig. 9(b). Note that the wall temperatures on both sides are not substantially amplified because of the short time heating of the laser. The temperature profiles for thick film behave like diffusion domination and are in accordance with theoretical results predicted by the classical heat-conduction theory.

4. Summary

A numerical study is performed on the effect of laser heating on the propagation phenomenon of a thermal wave in a very thin film subjected to a symmetrical heat source on both sides. The non-Fourier, hyperbolic heat conduction equation, which considers the laser radiation as a heat source, is solved using a numerical technique based on MacCormack's predictor–corrector scheme. Results have been obtained for the propagation process, magnitude and shape of thermal waves.

1. If a film is heated by the continuous-operated or pulsed lasers, temperature overshoot takes place in the films of smaller values of $x_0/2\tau c_0$ within a very short period of time. The effect of the laser heat source on the temperature distribution in the film becomes larger in the thin film. In other words, if the absorption coefficient, β, of the laser increases, the temperature is more dependent on the laser heat source in a thin film than in a thick film.
2. Overshoot and oscillation of thermal wave depend on the frequency ω of the heat source time characteristics.
3. As the dimensionless duration of the pulsed heat source Δ becomes larger, the temperature in the film is gradually increased over the whole cross-section of the film as the time progresses.

References

[1] K.J. Baumeister, T.D. Hamill, Hyperbolic heat conduction equation—a solution for the semi-infinite body problem, J. Heat Transfer 91 (1969) 543–548.
[2] S.H. Chan, M.J.D. Low, W.K. Mueller, Hyperbolic heat conduction in catalytic supported crystallites, AIChE J. 17 (1971) 1499–1501.
[3] M.S. Kazimi, C.A. Erdman, On the interface temperature of two suddenly contacting materials, J. Heat Transfer 97 (1975) 615–617.
[4] M.J. Maurer, H.A. Thompson, Non-Fourier effects at high heat flux, J. Heat Transfer 95 (1973) 284–286.
[5] B. Stritzker, A. Pospieszyk, J.A. Tagle, Measurement of lattice temperature of silicon during pulsed laser annealing, Phys. Rev. Lett. 47 (1981) 356–358.
[6] P. Baeri, S.U. Campisano, G. Foti, E. Rimini, A melting model for pulsing-laser annealing of implanted semiconductors, J. Appl. Phys. 50 (1979) 788–797.
[7] W.E. Maher, R.B. Hall, Pulsed laser heating profile width and changes in total coupling with pulse length and pressure, J. Appl. Phys. 51 (1980) 1338–1344.
[8] G.L. Eesley, Observation of non-equilibrium electron heating in copper, Phys. Rev. Lett. 51 (1983) 2140–2143.
[9] J.G. Fujimoto, J.M. Liu, E.P. Ippen, Femtosecond laser interaction with metallic tungsten and non-equilibrium electron and lattice temperatures, Phys. Rev. Lett. 53 (1984) 1837–1840.
[10] B. Vick, M.N. Ozisik, Growth and decay of a thermal pulse predicted by the hyperbolic heat conduction equation, J. Heat Transfer 105 (1983) 902–907.
[11] B.F. Blackwell, Temperature profile in semi-infinite body with exponential sources and convective boundary condition, J. Heat Transfer 112 (1990) 567–571.
[12] A.S. Zubair, M.A. Chaudhry, Heat conduction in a semi-infinite solid due to time-dependent laser source, Int. J. Heat Mass Transfer 39 (1996) 3067–3074.
[13] T.Q. Qiu, C.L. Tien, Short-pulse laser heating on metals, Int. J. Heat Mass Transfer 35 (1992) 719–726.
[14] D.Y. Tzou, The generalised lagging response in small-scale and high-rate heating, Int. J. Heat Mass Transfer 38 (1995) 3231–3240.
[15] L.G. Hector Jr., W.S. Kim, M.N. Ozisik, Hyperbolic heat conduction due to mode locked laser pulse train, Int. J. Engng. Sci. 30 (1992) 1731–1744.
[16] A. Kar, C.L. Chan, J. Mazumder, Comparative studies on nonlinear hyperbolic and parabolic heat conduction for various boundary conditions: analytical and numerical solutions, J. Heat Transfer 114 (1992) 14–20.
[17] M. Lewandowska, Hyperbolic heat conduction in the semi-infinite body with a time-dependent laser heat source, Heat Mass Transfer 37 (2001) 333–342.

[18] T.Q. Qiu, C.L. Tien, Size effect on nonequilibrium laser heating of metals, J. Heat Transfer 115 (1993) 842–847.
[19] M.N. Ozisik, D.Y. Tzou, On the wave theory in heat conduction, J. Heat Transfer 116 (1994) 526–535.
[20] M.N. Ozisik, B. Vick, Propagation and reflection of thermal waves in a finite medium, Int. J. Heat Mass Transfer 27 (1984) 1845–1854.
[21] D.W. Tang, N. Araki, On non-Fourier temperature wave and thermal relaxation time, Int. J. Thermophys. 18 (1997) 493–504.
[22] D.E. Glass, M.N. Ozisik, B. Vick, Hyperbolic heat conduction with surface radiation, Int. J. Heat Mass Transfer 28 (1985) 1823–1830.
[23] D.E. Glass, M.N. Ozisik, D.S. McRae, B. Vick, On the numerical solution of hyperbolic heat conduction, Numer. Heat Transfer 8 (1985) 497–504.
[24] D.A. Anderson, J.C. Tannehill, R.H. Pletcher, Computational Fluid Mechanics and Heat Transfer, Hemisphere, New York, 1983.
[25] J. Gembarovic, V. Majermik, Determination of thermal parameters of relaxation materials, Int. J. Heat Mass Transfer 30 (1987) 199–201.
[26] W. Walter, Change in reflectivity of metals under intense laser radiation, final Technical Report Microwave Research Institute, Polytechnic Institute, New York, AFOSR-TR-81-0567, 1980.